

## AN IMPROVED MODEL FOR SATURATED SALIENT POLE SYNCHRONOUS MOTORS

Joseph O. Ojo, Member, IEEE and Thomas A. Lipo, Fellow, IEEE  
 Department of Electrical and Computer Engineering  
 University of Wisconsin  
 Madison WI 53706

### ABSTRACT

An improved model for the transient analysis of saturated salient pole synchronous motors is presented. With the aid of saturation factors obtained by test or with finite elements, Park's equations for a synchronous machine are modified to independently account for the saturation of the d and q-axis magnetizing flux linkages in the region of the stator teeth and rotor pole face as well as saturation of the total flux linking the stator core. The model is used to calculate the starting performance for a direct on line start as well as the transient performance during a load change. These transients are correlated with both test results and the results predicted by a traditional model employing only d-axis main flux saturation. The new model shows improvement over more traditional models indicating that representation of both main flux and core saturation are important for synchronous machine analysis. Keywords: Saturation, Synchronous Motors, Starting, Torque.

### INTRODUCTION

The useful life of industrial synchronous motors are dependent on many factors including ambient temperature, severity of over and under voltages and voltage imbalances. An important practical concern is the starting phase of the industrial drive motor operation during which time the motor accelerates to the steady state full speed. Because of the large inrush transient currents flowing into the motor during the starting conditions (which result in heating of the motor windings) many large industrial drives are protected to prevent the motor from repetitive starting beyond specified limits. Such concerns are particularly important in applications where the motor is required to carry high inertia loads at starting as in the cases of pump loads and compressors.

During the starting interval, the transient currents generate double slip frequency pulsating torques. In a complex mechanical drive application, the mechanical system can have numerous resonance frequencies lying between zero and twice the supply frequency. If these resonance frequencies coincide with the pulsating torque frequency of the motor, severe torsional oscillations can result which can lead to coupling shearing and shaft breakage.

In view of the practical importance of the starting transient of synchronous motors, accurate methods to predict starting currents and the resulting electromagnetic torques are an essential application consideration. Relative to the recent activity in saturation modelling of induction machines, there has been little work done recently on saturation effects in synchronous machines. Over 30 years ago, Thomas [1] in discussing reference [2] derived an extended d-q-0 model of saturated synchronous machine which adjusted the main fluxes in the d and q axes for both steady and transient state operation. De Mello [3,4] took account of the saturation due to the field of the synchronous generator using an approach similar to that suggested by Thomas and obtained good

correlation between experimental and simulated results. Shackshaft [5] using a somewhat empirical method obtained equations for saturating mutual d and q axes reactances for salient pole synchronous machine. Assuming sinusoidal variation of permeance, the saturated mutual reactances are made functions of saturation factors and intersaturation terms. In a more recent paper Harley et al. [6], suggested a model for the saturated synchronous machine using d and q- saturation factors which are functions of the flux in their respective axes. With this model they show that for a micro alternator, saturation in the q-axis is important in the determination of the initial value of the load angle after short circuit faults. Ramshaw and Xie [7,8] have suggested models for round rotor and salient pole synchronous generators using the concepts of "static" and "dynamic" permeances to represent the saturation of the air gap flux. Accounting for saturation effects on the d-axis magnetizing path, they showed that for a line to ground fault on a line of a double circuit transmission line connected to a synchronous generator, the calculated power angle swing was reduced with the saturated model compared to the constant parameter model indicating greater critical clearing fault time for the saturated model.

Until recently, modelling of synchronous machine saturation was effectively limited to models in which the necessary saturation curves could be established by means of measurement. One of the traditional difficulties with the lumped saturation models heretofore used, is the fact that saturation occurs at different points within the machine for different modes of operation. For example, during normal load transients, the field current is relatively large and saturation is, to a great extent, limited to the region of rotor core under the field windings. Hence, a simple d-axis saturation model will adequately predict load transients provided the excursions are not too large. However, during the starting process, the field flux is relatively small and saturation primarily occurs in the stator core. In addition, the maximum core flux is dependent on the vector sum of the total d- and q-axes flux so that construction of an appropriate saturation function in a rotating d-q axes must be implemented in an entirely different manner. It is therefore clear, that when accuracy is desired during both conditions with a single model or when a solution is required during the period between these two conditions, i.e. during the pull in interval, conventional models continue to be lacking. However, with the advent of finite elements, analytical methods have improved to the point where machine parameters can be calculated with complete reliability. Hence, in the view of the authors, the time has arrived to look beyond models restricted by experimental limitations and develop new models, which, accompanied by finite element calculations, may improve computational accuracy.

In this paper a new equivalent circuit model is presented which can utilize finite elements for the computation of the circuit parameters [9]. The model accounts for the saturation effects in the stator core, rotor core, as well as stator teeth and rotor pole face, using separate saturation factors. The saturation factors inherently account for intersaturation phenomena between the d and q axes since they are defined in a general manner as functions of the total flux linkages depending on the data determined from a finite element model. The modelling approach proposed in this paper combines the advantages of the finite element method for parameter determination and the simplicity of the equivalent circuit approach making it more attractive in terms of computational time compared to other methods that solve the complete magnetic circuit at every time step [10]. The derivation of the d-q equations of the synchronous machine in the rotor reference frame accounting for the instantaneous spatial saturation effects is the theme of this paper.

88 SM 614-0 A paper recommended and approved by the IEEE Rotating Machinery Committee of the IEEE Power Engineering Society for presentation at the IEEE/PES 1988 Summer Meeting, Portland, Oregon, July 24 - 29, 1988. Manuscript submitted February 1, 1988; made available for printing May 27, 1988.

### MAGNETIC CIRCUIT MODEL

The concept of topological duality is frequently used to obtain the electric equivalent circuits of the machine from the magnetic equivalent circuits. This approach has an advantage over the usual method of deriving the electric equivalent circuit which relies on the concept of mutual coupling between windings in that the effects of magnetic nonlinearity can be easily represented. The stator and rotor windings can then be transformed into equivalent mutually perpendicular d and q windings from which the magnetic equivalent circuit for each axis is obtained. The MMF due to the currents flowing in the d and q-axes windings are consumed in the end winding and slot leakage parts, air gap, teeth, pole faces and the stator and rotor cores and can be accounted for independently if necessary.

The magnetic equivalent circuit assumed in this paper is shown in Fig. 1(a) for the equivalent d-axis magnetic circuit. It should be noted that this circuit is similar to that of Slemon [11]. Slemon's model, however, was used only for steady-state analysis and, when ultimately implemented, was reduced to a conventional lumped d-q-axis saturation model. In Fig. 1(a) the reluctance  $R_{sa}$  represents the reluctance due to stator flux linkages which are essentially in air and effectively correspond to the end winding flux linkages [12]. The reluctance  $R_{sb}$  represents the stator leakage flux linkages which have an iron path, i.e. the slot, harmonic and tooth top leakages.  $R_{sc}$  is the reluctance corresponding to the permeance of the stator core. The MMF drop across this reluctance is, in fact, assumed to result from the vector sum of the q and d-axis core flux linkages rather than the d-axis flux alone as implied by Fig. 1(a). The quantity  $R_{md}$  is the reluctance associated with mmf drop across the stator tooth, air gap as well as rotor pole. The corresponding equivalent electric circuit is obtained essentially from the circuit dual of Fig. 1(a) and is shown in Fig. 1(b). The same approach of derivation of the d-axis equivalent circuit is also used for the q-axis windings.

### SIMULATION EQUATIONS ACCOUNTING FOR SATURATION EFFECTS

Figure 2 shows the complete equivalent d-q circuit model which follows from the electric circuit model of Fig. 1(b) and conventional d-q analysis [13]. In the following analysis both the saturation of the stator core ( $L_{sc}$ ) and the stator teeth and field pole ( $L_{md}, L_{mq}$ ) are considered. In general, the inductances  $L_{sb}$ ,  $L_{qrb}$ , and  $L_{drb}$  can also saturate. However, for the machine studied in this paper this inductance can be assumed as constant.

In order to simulate the machine with the minimum amount of computational effort it is important to avoid so-called algebraic loops. The approach taken in this paper follows that of Ref 12. From Fig. 2 the well known d-q voltage equations in the rotor reference frame remain as follows:

$$v_{qs} = r_s i_{qs} + \frac{p}{\omega_b} \psi_{qs} + \frac{\omega_r}{\omega_b} \psi_{ds} \quad (1)$$

$$v_{ds} = r_s i_{ds} + \frac{p}{\omega_b} \psi_{ds} - \frac{\omega_r}{\omega_b} \psi_{qs} \quad (2)$$

$$v_{kq} = r_{kq} i_{kq} + \frac{p}{\omega_b} \psi_{kq} \quad (3)$$

$$v_{kd} = r_{kd} i_{kd} + \frac{p}{\omega_b} \psi_{kd} \quad (4)$$

$$v_{fd} = r_{fd} i_{fd} + \frac{p}{\omega_b} \psi_{fd} \quad (5)$$

where  $p$  denotes the time derivative operator  $d/dt$  and  $v_{kd}$  and  $v_{kq}$  are zero.

In order to incorporate the effect of saturation the equations for the flux linkages are written as follows:

$$\psi_{qs} = X_{sa} i_{qs} + \psi_{qsc}(\text{sat}) \quad (6)$$

$$\psi_{qsc}(\text{sat}) = X_{sb} i_{qss} + \psi_{mq}(\text{sat}) \quad (7)$$

$$\psi_{ds} = X_{sa} i_{ds} + \psi_{dsc}(\text{sat}) \quad (8)$$

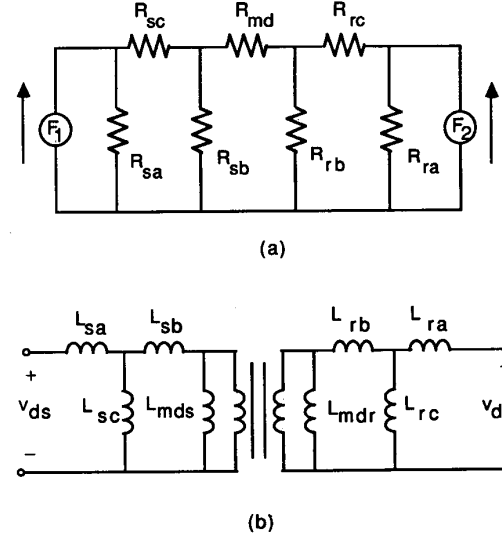


Fig. 1 (a) Magnetic and (b) Electric Equivalent Circuits of d-Axis Flux Components of a Synchronous Machine.

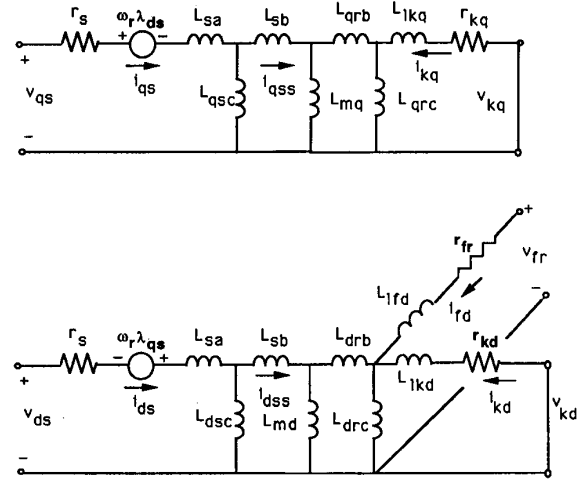


Fig. 2 d-q Equivalent Circuit of a Salient Pole Synchronous Machine.

$$\psi_{dsc}(\text{sat}) = X_{sb} i_{dss} + \psi_{md}(\text{sat}) \quad (9)$$

$$\psi_{kq} = X_{lkq} i_{kq} + \psi_{qrc}(\text{sat}) \quad (10)$$

$$\psi_{qrc}(\text{sat}) = X_{qrb} i_{qrr} + \psi_{mq}(\text{sat}) \quad (11)$$

$$\psi_{kd} = X_{lkd} i_{kd} + \psi_{drc}(\text{sat}) \quad (12)$$

$$\psi_{drc}(\text{sat}) = X_{drb} i_{drr} + \psi_{md}(\text{sat}) \quad (13)$$

$$\psi_{fd} = X_{lfd} i_{fd} + \psi_{drc}(\text{sat}) \quad (14)$$

where, the flux linkages  $\lambda_{qs}$ , and  $\lambda_{ds}$ , have, in conventional fashion [14], been multiplied by a constant base frequency  $\omega_b$  to yield the d-q stator flux linkages  $\psi_{qs}$ ,  $\psi_{ds}$  having units of volts.

The quantities  $\Psi_{qsc}$ ,  $\Psi_{dsc}$  and  $\Psi_{qrc}$ ,  $\Psi_{drc}$  are the q, d stator core and rotor core flux linkages in volts respectively. The quantities  $\Psi_{kq}$ ,  $\Psi_{fd}$ , are the d-axis flux linkages for the damper and field windings respectively, and  $\Psi_{kq}$ , represents the q-axis damper flux linkages. From Eqs. (6) to (14), the following expressions are derived for the machine currents,

$$i_{qs} = [\Psi_{qs} - \Psi_{qsc}(\text{sat})] / X_{sa} \quad (15)$$

$$i_{ds} = [\Psi_{ds} - \Psi_{dsc}(\text{sat})] / X_{sa} \quad (16)$$

$$i_{qss} = [\Psi_{qsc}(\text{sat}) - \Psi_{mq}(\text{sat})] / X_{sb} \quad (17)$$

$$i_{dss} = [\Psi_{dsc}(\text{sat}) - \Psi_{md}(\text{sat})] / X_{sb} \quad (18)$$

$$i_{kq} = [\Psi_{kq} - \Psi_{qrc}(\text{sat})] / X_{lkq} \quad (19)$$

$$i_{kd} = [\Psi_{kd} - \Psi_{drc}(\text{sat})] / X_{lkd} \quad (20)$$

$$i_{fd} = [\Psi_{fd} - \Psi_{drc}(\text{sat})] / X_{lfd} \quad (21)$$

$$i_{qrr} = [\Psi_{qrc}(\text{sat}) - \Psi_{mq}(\text{sat})] / X_{qrb} \quad (22)$$

$$i_{drr} = [\Psi_{drc}(\text{sat}) - \Psi_{md}(\text{sat})] / X_{drb} \quad (23)$$

In Eqs. (15) to (23), the inductances have been replaced by equivalent reactances i.e.,

$$X_{lkq} = \omega_b L_{lkq} \quad (24)$$

and, so forth for the air dependant d-axis leakage reactance  $X_{lkd}$ , the field leakage reactance  $X_{lfd}$ , the stator iron dependent leakage reactance  $X_{sb}$  and the stator air dependent leakage reactance  $X_{sa}$  and the rotor iron dependant leakage reactances  $X_{drb}$  and  $X_{qrb}$ . It is important to note that the leakage inductances in Eqs. 15-23 are all linear so that division by non-linear quantities is completely avoided and the computational effort to solve the system equations is greatly reduced.

The currents  $i_{qs}$ ,  $i_{ds}$  are the q and d currents flowing into the stator terminals,  $i_{qss}$ ,  $i_{dss}$ , denote q and d stator magnetizing currents,  $i_{kq}$ ,  $i_{kd}$ , are the rotor q and d currents flowing in the damper windings,  $i_{fd}$ , is the rotor field current and  $i_{qrr}$ ,  $i_{drr}$  are the d,q rotor magnetizing currents.

When the current equations are substituted in equations (1) to (5), the following flux equations result:

$$\frac{p}{\omega_b} \Psi_{qs} = v_{qs} + \frac{r_s}{X_{sa}} (\Psi_{qsc}(\text{sat}) - \Psi_{qs}) - \frac{\omega_r}{\omega_b} \Psi_{ds} \quad (25)$$

$$\frac{p}{\omega_b} \Psi_{ds} = v_{ds} + \frac{r_s}{X_{sa}} (\Psi_{dsc}(\text{sat}) - \Psi_{ds}) + \frac{\omega_r}{\omega_b} \Psi_{qs} \quad (26)$$

$$\frac{p}{\omega_b} \Psi_{kq} = v_{kq} + \frac{r_{kq}}{X_{lkq}} (\Psi_{qrc}(\text{sat}) - \Psi_{kq}) \quad (27)$$

$$\frac{p}{\omega_b} \Psi_{kd} = v_{kd} + \frac{r_{kd}}{X_{lkd}} (\Psi_{drc}(\text{sat}) - \Psi_{kd}) \quad (28)$$

$$\frac{p}{\omega_b} \Psi_{fd} = v_{fd} + \frac{r_{fd}}{X_{lfd}} (\Psi_{drc}(\text{sat}) - \Psi_{fd}) \quad (29)$$

The unsaturated magnetizing flux in the d and q axes are given as:

$$\Psi_{mq}(\text{unsat}) = X_{mq} (i_{qss} + i_{qrr}) \quad (30)$$

$$\Psi_{md}(\text{unsat}) = X_{md} (i_{dss} + i_{drr}) \quad (31)$$

The saturated d-q flux of the magnetizing branch is given as:

$$\Psi_{mq}(\text{sat}) = \Psi_{mq}(\text{unsat}) - \Delta\Psi_{mq} \quad (32)$$

$$\Psi_{md}(\text{sat}) = \Psi_{md}(\text{unsat}) - \Delta\Psi_{md} \quad (33)$$

$$\Delta\Psi_{mq} = (1 - K_{mq}) \Psi_{mq}(\text{unsat}) \quad (34)$$

$$\Delta\Psi_{md} = (1 - K_{md}) \Psi_{md}(\text{unsat}) \quad (35)$$

where,  $K_{md}$ ,  $K_{mq}$  are the saturation factors for the d and q-axis magnetizing fluxes which are function of the total q and d-axis unsaturated magnetizing flux linkages given as:

$$\Psi_m(\text{unsat}) = \sqrt{\Psi_{mq}^2(\text{unsat}) + \Psi_{md}^2(\text{unsat})} \quad (36)$$

and,  $\Delta\Psi_{md}$ ,  $\Delta\Psi_{mq}$  are changes in the flux levels from the unsaturated values in the d and q axes respectively.

When the currents in Eqs. (15) to (23) are substituted in Eqs. (30) and (31),

$$\begin{aligned} \Psi_{mq}(\text{unsat}) = X_{mq} \left[ \frac{\Psi_{qsc}}{X_{sb}} + \frac{\Psi_{qrc}}{X_{qrb}} \right] \\ + X_{mq} \left( \frac{1}{X_{sb}} + \frac{1}{X_{qrb}} \right) \Delta\Psi_{mq} \end{aligned} \quad (37)$$

$$\begin{aligned} \Psi_{md}(\text{unsat}) = X_{md} \left[ \frac{\Psi_{dsc}}{X_{sb}} + \frac{\Psi_{drc}}{X_{drb}} \right] \\ + X_{md} \left( \frac{1}{X_{sb}} + \frac{1}{X_{drb}} \right) \Delta\Psi_{md} \end{aligned} \quad (38)$$

where,

$$X_{mdd} = 1 / \left( \frac{1}{X_{md}} + \frac{1}{X_{sb}} + \frac{1}{X_{drb}} \right) \quad (39)$$

$$X_{mq} = 1 / \left( \frac{1}{X_{mq}} + \frac{1}{X_{sb}} + \frac{1}{X_{qrb}} \right) \quad (40)$$

The unsaturated core fluxes are given as:

$$\Psi_{qsc}(\text{unsat}) = X_{sc} (i_{qs} - i_{qss}) \quad (41)$$

$$\Psi_{dsc}(\text{unsat}) = X_{sc} (i_{ds} - i_{dss}) \quad (42)$$

$$\Psi_{qrc}(\text{unsat}) = X_{rc} (i_{kq} - i_{qrr}) \quad (43)$$

$$\Psi_{drc}(\text{unsat}) = X_{rc} (i_{kd} + i_{fd} - i_{drr}) \quad (44)$$

Substituting the expressions for the currents in the equations above it can be shown finally that,

$$\begin{aligned} \Psi_{dsc}(\text{unsat}) = X_{sc} \left[ \left( \frac{\Psi_{ds}}{X_{sa}} + \frac{\Psi_{md}}{X_{sb}} \right) \right. \\ \left. + \left( \frac{1}{X_{sa}} + \frac{1}{X_{sb}} \right) \Delta\Psi_{dsc} \right] \end{aligned} \quad (45)$$

$$\begin{aligned} \Psi_{qsc}(\text{unsat}) = X_{sc} \left[ \left( \frac{\Psi_{qs}}{X_{sa}} + \frac{\Psi_{mq}}{X_{sb}} \right) \right. \\ \left. + \left( \frac{1}{X_{sa}} + \frac{1}{X_{sb}} \right) \Delta\Psi_{qsc} \right] \end{aligned} \quad (46)$$

$$\Psi_{drc(unsat)} = X_{drc} \left[ \frac{\Psi_{kd}}{X_{lkd}} + \frac{\Psi_{fd}}{X_{lfd}} + \frac{\Psi_{md(sat)}}{X_{drb}} \right] + \Delta\Psi_{drc} \left[ \frac{1}{X_{lkd}} + \frac{1}{X_{lfd}} + \frac{1}{X_{drb}} \right] X_{drc} \quad (47)$$

$$\Psi_{qrc(unsat)} = X_{qrc} \left[ \frac{\Psi_{kq}}{X_{lkq}} + \frac{\Psi_{mq(sat)}}{X_{qrb}} \right] + \Delta\Psi_{qrc} \left[ \frac{1}{X_{lkq}} + \frac{1}{X_{qrb}} \right] X_{qrc} \quad (48)$$

where,

$$X_{scc} = 1 / \left( \frac{1}{X_{sc}} + \frac{1}{X_{sa}} + \frac{1}{X_{sb}} \right) \quad (49)$$

$$X_{drc} = \left( \frac{1}{X_{drc}} + \frac{1}{X_{lkd}} + \frac{1}{X_{lfd}} + \frac{1}{X_{drb}} \right)^{-1} \quad (50)$$

$$X_{qrc} = \left( \frac{1}{X_{qrc}} + \frac{1}{X_{lkq}} + \frac{1}{X_{qrb}} \right)^{-1} \quad (51)$$

The changes in the d and q axes flux linkages in the core due to saturation are now given as

$$\Delta\Psi_{qsc} = (1-K_s)\Psi_{qsc}(unsat) \quad (52)$$

$$\Delta\Psi_{dsc} = (1-K_s)\Psi_{dsc}(unsat) \quad (53)$$

$$\Delta\Psi_{qrc} = (1-K_{qr})\Psi_{qrc}(unsat) \quad (54)$$

$$\Delta\Psi_{drc} = (1-K_{dr})\Psi_{drc}(unsat) \quad (55)$$

Whereupon the saturated d and q core flux linkages can be written as,

$$\Psi_{qsc}(sat) = \Psi_{qsc}(unsat) - \Delta\Psi_{qsc} \quad (56)$$

$$\Psi_{dsc}(sat) = \Psi_{dsc}(unsat) - \Delta\Psi_{dsc} \quad (57)$$

$$\Psi_{qrc}(sat) = \Psi_{qrc}(unsat) - \Delta\Psi_{qrc} \quad (58)$$

$$\Psi_{drc}(sat) = \Psi_{drc}(unsat) - \Delta\Psi_{drc} \quad (59)$$

The quantities  $\Delta\Psi_{qsc}$ ,  $\Delta\Psi_{dsc}$  and  $\Delta\Psi_{qrc}$ ,  $\Delta\Psi_{drc}$  are changes in the flux linkages in the q and d axes due to saturation in the stator and rotor cores. The parameter  $K_s$  is the saturation factor for the stator core and is a function of the total unsaturated stator core flux linkage,

$$\Psi_{sc}(unsat) = \sqrt{\Psi_{qsc}^2(unsat) + \Psi_{dsc}^2(unsat)} \quad (60)$$

The rotor saturation factors  $K_{dr}$  and  $K_{qr}$  are defined in a similar manner.

The electromagnetic torque of a machine with a number of poles P is then given as,

$$T_e = \frac{3}{2} \frac{P}{(2\omega_p)} (\Psi_{ds} i_{qs} - \Psi_{qs} i_{ds}) \quad (61)$$

Finally, the equation of motion for the synchronous motor can be written

$$J \frac{\omega_r}{dt} = T_e - T_l \quad (62)$$

In summary, Eqs. (25) to (62) are the equations to be solved for the performance of the saturated salient pole synchronous machine with saturation effects in the poles, tooth and in the stator core. A simulation block diagram for the d-axis flux linkages corresponding to these equations is shown in Fig. 3. The q-axis flux linkages are obtained in a similar manner. The simulation for the machine currents, torque and speed follow conventional procedures. It is important to note that the effects of saturation have been isolated in three simple non-linear blocks.

### DETERMINATION OF SYNCHRONOUS MOTOR PARAMETERS

In general, conventional approaches has been followed to determine the parameters of the test machine and not finite elements. The parameters of the test motor are shown in Appendix A. For the implementation of the proposed model, a special method for the determination of the unconventional parameters was designed. The test machine was mechanized with search coils in the air gap, the stator slot and around the stator core for the measurement of induced voltages under varying load, stator terminal and field voltages. The measured induced voltages, terminal voltages, currents, load and power factor angles were used to calculate the stator core, rotor core, q and d magnetizing reactances and their corresponding saturation factors for varying degrees of excitation of field currents. This method of parameter determination [3] based on actual data collected in the operability region of the machine, as opposed to the use of no load and short circuit tests has the potential of capturing the interactive effects of the field and the stator flux linkages and the intersaturation phenomena between the q and d axes. Figures 4 through 6 show the saturation factors for the d and q-axis magnetizing fields and the stator core. It was determined through test that the rotor was not appreciably saturated so that the rotor saturation factors  $K_{dr}$  and  $K_{qr}$  were set equal to 1.0. Also, for the test motor, the d-axis reactance and the saturation factor was independent of the q-axis flux linkages while the q-axis reactance and saturation factor depend on the total magnetizing field flux linkages. Admittedly the parameter determination method followed in this work is tedious but finite element analysis methods can be used to determine these parameters by using measured currents as inputs to the programs [9]. However, in [13], a detailed description of both the experimental and finite element method approaches are laid out for the determination of the machine parameters.

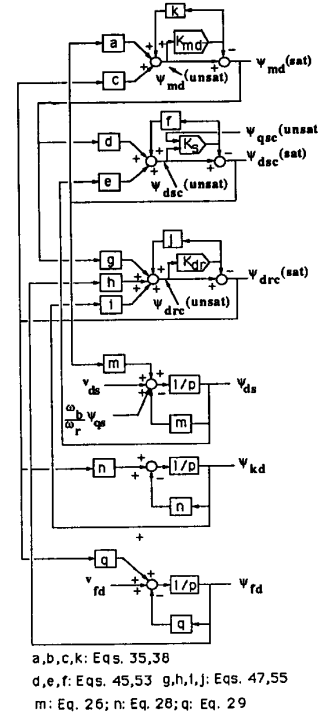


Fig. 3 Simulation Diagram for d-Axis of Salient Pole Synchronous Machine Including Stator Core, Rotor Core and Main Flux Saturation Effects.

**STARTING OF SALIENT POLE SYNCHRONOUS MOTOR**

In order to verify the usefulness of the proposed model (model I), simulation has been implemented for the starting of a three phase, three wire 208 V salient pole synchronous motor rated at 25 HP without connected load. For comparison purposes a simulation of the conventional model which considers only main flux d-axis saturation (model II) has also been carried out. Figure 7 shows the speed profiles of the free acceleration run up condition for the two models together with the measured experimental result. The measured run up time is 0.66 seconds which compares to the computed time of 0.64 second for model (I). The constant parameter model gave run up time of 0.72 seconds. Figure 8 shows the corresponding computed and measured electromagnetic torque. A close correlation between the prediction of model (I) and the measured developed torque can be noted. The d-axis saturation model II clearly predicts less developed torque at starting. Figure 9

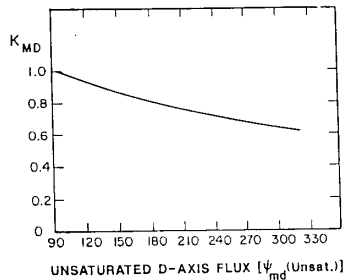


Fig. 4 Saturation Factor for the Magnetizing d-Axis Main Flux as a Function of the Unsaturated d-Axis Main Magnetizing Flux.

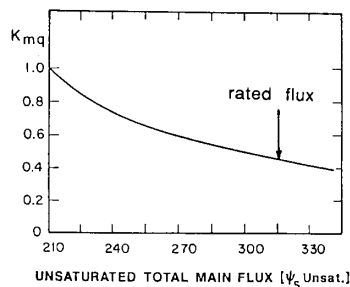


Fig. 5 Saturation Factor for the Magnetizing q-Axis Main Flux as a Function of the Unsaturated q-Axis Main Magnetizing Flux.

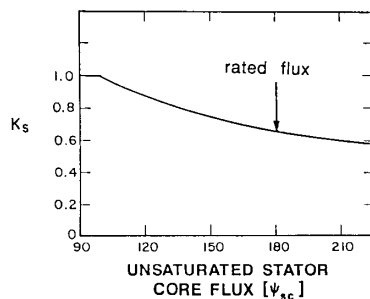


Fig. 6 Saturation Factor for the Stator Core Flux as a Function of the Total Unsaturated Core Flux.

also shows the phase "a" stator current and again a good correlation can be seen between the calculated result from model (I) and the measured current with each indicating a peak current of almost 500 amperes. Figure 10 shows the field current during the run up time. The profile and the magnitude of this current computed by model (I) and the measured profile are very much the same. Note that the d-axis main flux saturation model has a higher initial field current compared to the measured value.

In general it is evident from the above comparisons that accounting for the magnetizing field and core saturation in the analysis of the synchronous machine has an important effect on the run up time, the starting torques and currents. The d-axis saturation model tends to give results which are on the low side for the starting currents and torque and yields a longer run up time.

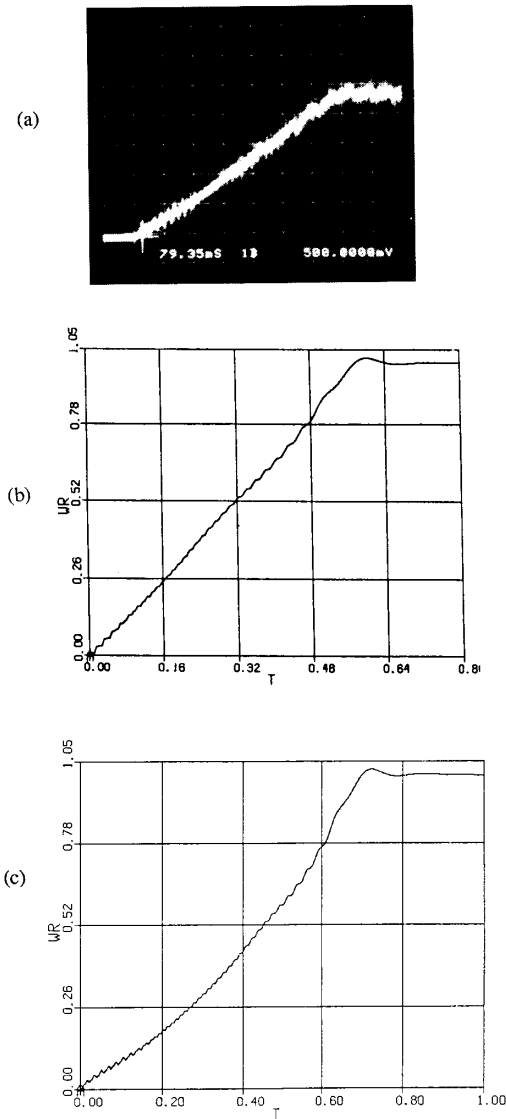


Fig. 7 Starting Transient of Salient Pole Synchronous Motor Showing Run Up Speed. (a) Experimental Results. Scale: 240 RPM/div., Time: 80 ms/div., (b) Model I with Saturation in Stator Core and d-q Magnetizing Branches, (c) Model II with Saturation only in d-Axis Magnetizing Branch.

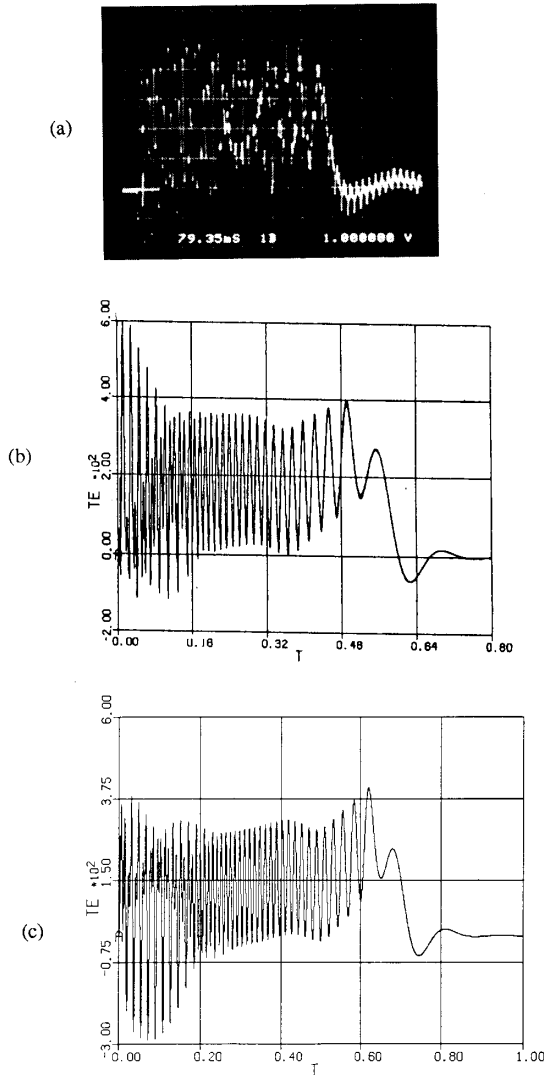


Fig. 8 Starting Transient of Salient Pole Synchronous Motor Showing Electromagnetic Torque. (a) Experimental Results, Scale: 125 Nm/div, Time: 80 ms/div, (b) Model I with Saturation in Stator Core and d-q Magnetizing Branches, (c) Model II with Saturation only in d-Axis Magnetizing Branch.

#### BEHAVIOR OF MOTOR WITH CHANGE IN LOAD TORQUE

Under starting conditions most of the saturation occurs in the stator core so that to a first approximation saturation can be neglected in the d and q-axis magnetizing inductances. It is therefore important to test the model when the motor is loaded with some excitation in the field so that air gap flux linkages in the d and q-axis are substantial. For this purpose, the experimental motor was loaded with a torque of 150 Nm with 115 Volts excitation voltage corresponding to approximately unity power factor and after a long time of steady state operation, the load is suddenly rejected. The loading and rejection was simulated using models (I) and (II). Figure 11 illustrates the measured and simulated developed torque profiles after the load was rejected. There is a

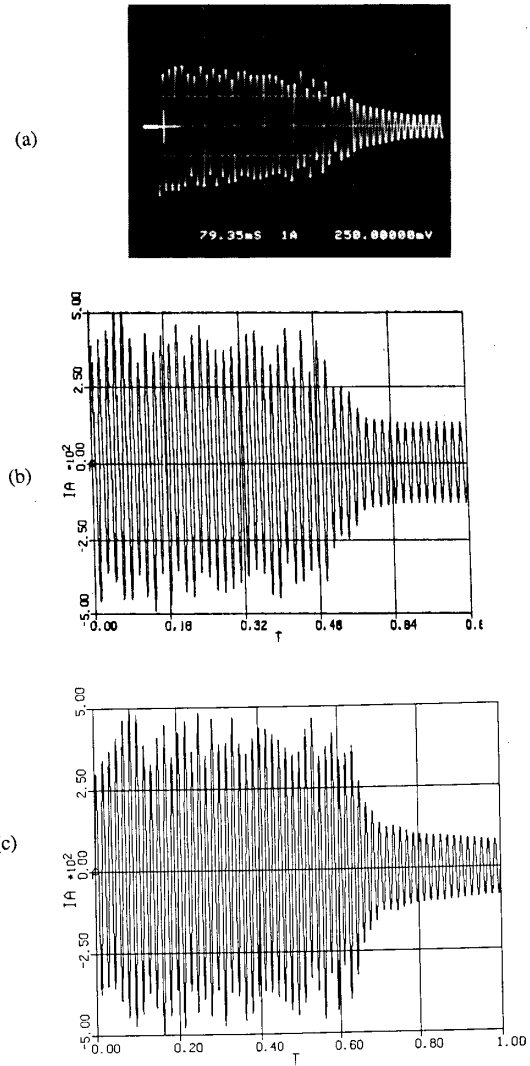


Fig. 9 Starting Transient of Salient Pole Synchronous Motor Showing Phase a Stator Current. (a) Experimental Results, Scale: 250 A/div, Time: 80 ms/div., (b) Model I with Saturation in Stator Core and d-q Magnetizing Branches, (c) Model II with Saturation only in d-Axis Magnetizing Branch.

close correlation between the measured and the simulated result of model (I) particularly in the settling time. Figure 12 (a) shows the measured phase 'a' current which compares very well in magnitude and profile to that predicted by the new model shown in Fig. 12 (b). The d-axis saturation model predicts slightly less steady state current as illustrated in Fig. 12 (c). It can be noted that the difference between the two models is not substantial in this case, which is to be expected since the good accuracy of d-axis saturation model under such conditions is widely accepted.

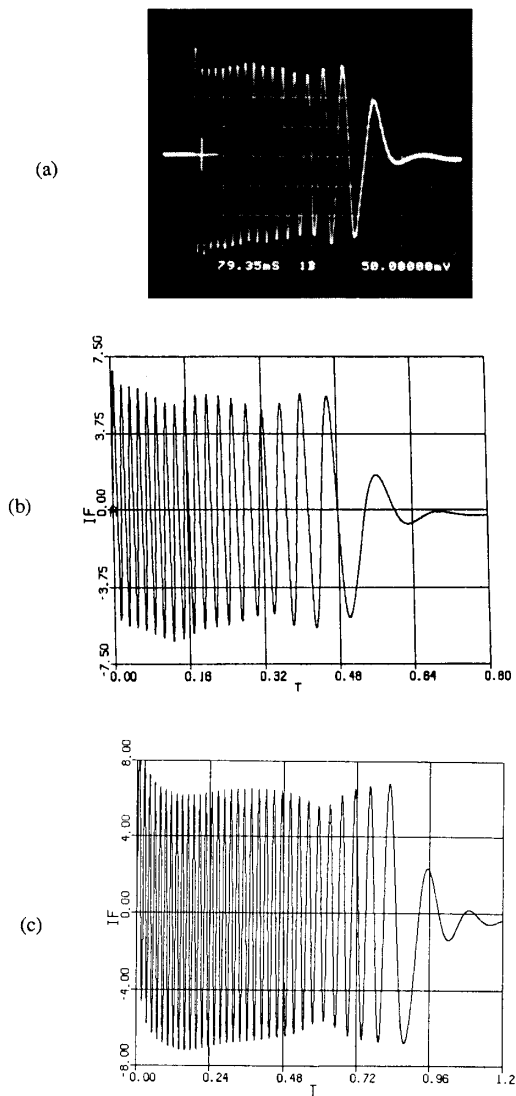


Fig. 10 Starting Transient of Salient Pole Synchronous Motor Showing Excitation Field Current. (a) Experimental Results, Scale: 2 A/div, Time: 80 ms/div., (b) Model I with Saturation in Stator Core and d-q Magnetizing Branches, (c) Model II with Saturation only in d-Axis Magnetizing Branch.

### CONCLUSION

Simulation and test results have indicated that for accurate computation for both synchronous and asynchronous operation of a salient pole synchronous machine performance the saturation effects in the stator core as well as magnetizing flux should be considered. Models neglecting stator core saturation will give good results only during low voltage starting. The influence of the field core saturation is most felt in the steady state when it is in a deeply saturated condition.

### ACKNOWLEDGMENTS

The authors are indebted to the industrial sponsors of the Wisconsin Electric Machines and Power Electronics Consortium (WEMPEC) for partial support of this work. The authors also wish to thank Prof. V. Ostovic for helping with the laboratory instrumentation.

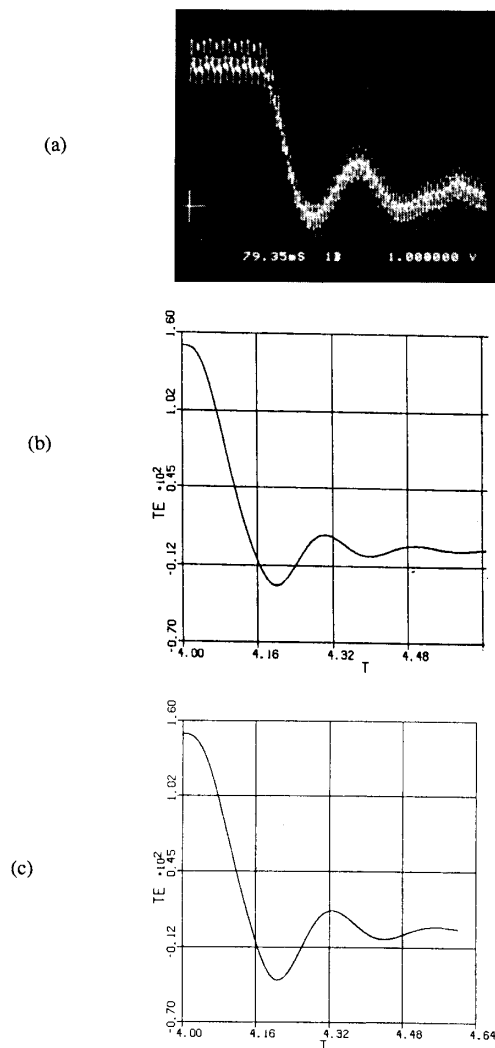


Fig. 11 Performance of Salient Pole Synchronous Motor During Step Unload. Trace Shows Electromagnetic Torque, (a) Experimental Results, Scale: 30 Nm/div, Time: 80 ms/div., (b) Model I with Saturation in Stator Core and d-q Magnetizing Branches, (c) Model II with Saturation only in d-Axis Magnetizing Branch.

### REFERENCES

- [1] C.H Thomas, Discussion of Reference [2], Trans. AIEE, Vol 75, pp. 1185, December 1956.
- [2] M. Riaz, "Analogue Computer Representation of Synchronous Generators in Voltage - Regulation Studies", Trans. AIEE, Vol. 75, pp. 1178 - 1184, December 1956.
- [3] F.P de Mello and J.R Ribeiro, "Derivation of synchronous Machine Parameters From Tests", IEEE Trans. on Power Apparatus and Systems, Vol PAS - 96, No 4, July / August 1977, pp. 1211-1218.
- [4] F.P de Mello and L.N Hannett, "Representation of Saturation in Synchronous Machines", IEEE Trans. on Power Systems, Vol. PWRS - 1, No. 4, November 1986, pp. 8-18.
- [5] Shackshaft G, "Data Requirement", Presented at the Symposium on Power System Dynamics, UMIST, Manchester England, 1973.

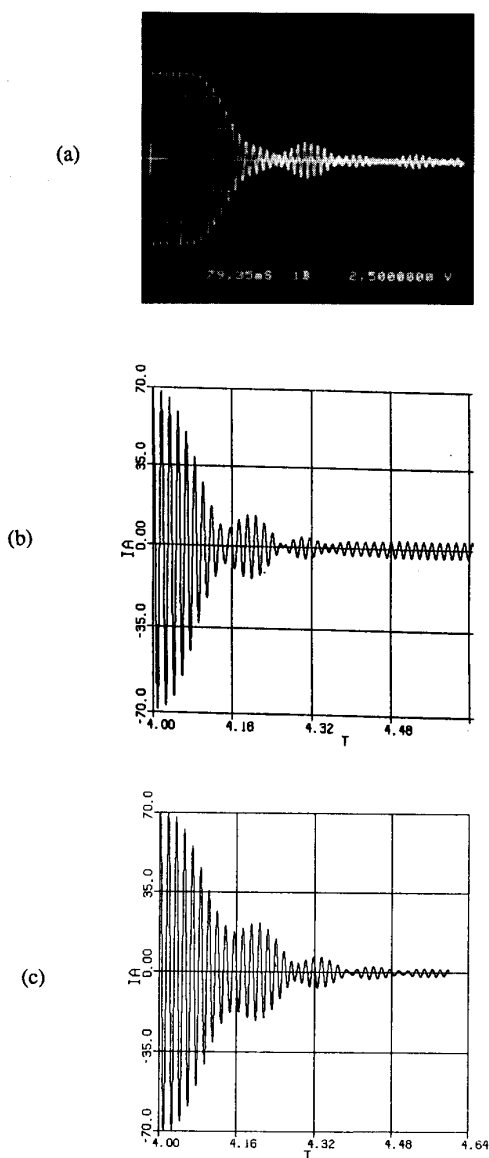


Fig. 12 Performance of Salient Pole Synchronous Motor During Step Unload. Phase *a* Current, (a) Experimental Results, Scale 30 Nm/div, Time 80 ms/div., (b) Model I with Saturation in Stator Core and d-q Magnetizing Branches, (c) Model II with Saturation only in d-Axis Magnetizing Branch.

- [6] Harley R.G, Limebeer D.J.N and Chirricozzi E, "Comparative Study of Saturation Methods in Synchronous Machine Models", IEE Proc. Vol. 127, Part B, No.1, January 1980, pp. 1- 6.
- [7] R.S Ramshaw and G. Xie, "Non Linear Model of Nonsalient Synchronous Machines", IEEE Trans. on Power Apparatus and System, Vol. PAS. 131, 1984, pp. 1809 - 1815.
- [8] G. Xie and R.S Ramshaw, "Nonlinear Model of Synchronous Machine with Saliency", Trans. IEEE Trans. on Energy Conversion, Vol. EC -1, No. 3, September 1986, pp. 198 - 203.
- [9] S.H. Minnich, R.P. Schulz, D.K. Baker, D.K. Sharma, R.G. Farmer and J.H. Fish, "Saturation Functions for Synchronous Generators from Finite Elements", IEEE Power

Engineering Society Conference, Winter 1987, Paper No. 87 WM 207 - 4.

- [10] M.P. Krefia and O. Wasynczuk O, "A Finite Element Based State Model of Solid Rotor Synchronous Machines", IEEE Transactions on Energy Conversion, Vol. EC - 2, No. 1, March 1987, pp. 21 - 30.
- [11] G.R. Slemon G.R, "Analytical Models for Saturated Synchronous Machines", IEEE Trans. on Power Apparatus and Systems, Vol. 2, March / April 1971, pp. 409 - 417.
- [12] T.A. Lipo and A. Consoli, "Modelling and Simulation of Induction motors with Saturable Leakage Reactances", IEEE Trans. on Industry Applications, Vol. IA - 20, No. 1, January / February 1984, pp. 180 - 189.
- [13] J.O. Ojo, "Saturation Effects in Alternating Current Electric Machines", Ph.D. Thesis, University of Wisconsin-Madison, 1987.
- [14] Krause P.C, Analysis of Electric Machinery, (Book), McGraw - Hill Book Company, New York, 1986.

#### APPENDIX A PARAMETERS OF TEST SYNCHRONOUS MACHINE

The synchronous motor used for the simulations is a 25 HP, 6 pole, salient pole synchronous motor rated at 208 volts line to line and rated current of 58 amperes. The rated field current is 3.8 amperes and requires an excitation voltage of 125 volts for unity power factor operation at rated load. The parameters of the test synchronous machine are as follows:

Stator resistance per phase,  $r_s = 0.0667 \Omega$

Q-axis damper resistance referred to the stator,  $r_{kq} = 0.0904 \Omega$

D-axis damper resistance referred to the stator,  $r_{kd} = 0.0993 \Omega$ .

Rotor field resistance referred to the stator,  $r_{fd} = 0.017 \Omega$ .

Stator end- winding reactance per phase,  $X_{sa} = 0.0606 \Omega$ .

Stator slot leakage reactance per phase,  $X_{sb} = 0.0606 \Omega$ .

Stator core reactance per phase,  $X_{sc} = 38.25 \Omega$ .

Unsaturated d-axis magnetizing reactance/phase,  $X_{md} = 1.62 \Omega$ .

Unsaturated q-axis magnetizing reactance/phase,  $X_{mq} = 1.09 \Omega$ .

Rotor field leakage reactance  $X_{lfd}$  (referred to stator) = 0.6291  $\Omega$

q-axis damper winding leakage reactance,  $X_{kq} = 0.594 \Omega$ .

d-axis damper winding leakage reactance,  $X_{kd} = 0.574 \Omega$ .

Inertia of the motor without connected load,  $J = 1.10 \text{ kg m}^2$

#### BIOGRAPHIES

J.O. Ojo (M'87) received the B.Eng. and M.Eng. Degrees in Electrical Engineering from Ahmadu Bello University (ABU) Zaria, Nigeria in 1977 and 1982 respectively and the Ph.D. degree from the University of Wisconsin-Madison in 1987. He was a lecturer in ABU from 1978 to 1982 and presently is a postdoctoral fellow at the University of Wisconsin-Madison. His fields of interest are energy conversion, control and power electronics.

Thomas A. Lipo (M'64-SM'71-F'87) received his B.E.E. and M.S.E.E. degrees from Marquette University, Milwaukee, WI, in 1962 and 1964 respectively, and the Ph.D. degree in electrical engineering from the University of Wisconsin in 1968.

From 1969 to 1979 he was an Electrical Engineer in the Power Electronics Laboratory of Corporate R&D, General Electric Co. He is presently Professor in the Department of Electrical and Computer Engineering, University of Wisconsin-Madison. His special interests are electrical machines and power electronics. He is an active member of 5 IEEE Committees or Subcommittees (past Chairman of two). He is a member of the Executive Board of the Industrial Applications Society, AdCom Member of the Power Electronics Society and Editor of the IEEE Transactions on Power Electronics.